Magnetic properties of gadolinium and terbium nanoparticles produced via multilayer precursors

Z. C. Yan, Y. H. Huang, Y. Zhang, H. Okumura, J. Q. Xiao, S. Stoyanov, V. Skumryev, and G. C. Hadjipanayis
Department of Physics and Astronomy, University of Delaware, Newark, Delaware 19716

C. Nelson
NCEM, Lawrence Berkeley National Laboratory, Berkeley, California 94720

(Received 25 March 2002; revised manuscript received 4 November 2002; published 5 February 2003)

Gd and Tb nanoparticles were obtained via annealing of sputtered multilayer precursors. Detailed structural examination, involving energy-filtered imaging and high-resolution electron microscopy along with transmission electron microscopy and scanning electron microscopy techniques, revealed an island structure for the rare earths within the precursors, which further develops to nanoparticles upon annealing. A dramatic change in the magnetic characteristics of the nanoparticles is observed comparing to the bulk. Magnetic data are discussed to distinguish between true size effects and superparamagnetism. The obtained results give a credit to the former scenario.

DOI: 10.1103/PhysRevB.67.054403 PACS number(s): 75.75.+a

I. INTRODUCTION

Rare-earth elements, alloys, and compounds form a unique group of materials with diverse properties. Magnetism in the rare-earths (RE) originates almost entirely from incomplete $4f$ shells which, being localized deep inside the atoms, are well screened by the surrounding electrons. The moments are coupled via an indirect exchange-coupling mechanism [Ruderman-Kittel-Kasuya-Yasida (RKKY)] involving the polarization of conduction electrons. The rich magnetism of rare-earth elements is still a challenging area of research.

Because the RKKY interactions are mediated by the valence electrons, they are very sensitive to the structure and filling of the conduction bands. Thus, small changes in the band structure of a solid, originating from nanosize, are expected to have dramatic effects on the magnetic properties. Furthermore, the large surface area of nanoparticles is expected to play a significant role on their magnetic properties.

It is surprising, but most of the research on nonbulk rare earths has been done on thin films (monolayers or multilayers)[1–7] or on clusters containing up to few tens of atoms[8–11] and very little on nanoparticles. The results, while intriguing, are also rather contradicting. Spin polarized low-energy electron diffraction experiments on ultrathin films[5] of Gd revealed a surface enhanced magnetic order (some 60 K above bulk T_c). However, other results contradict these findings.[6] The transition temperature of 5–100 ML of Gd was found to decrease with reducing the layer thickness, while the anisotropy increased.[7] Gd clusters ($N=11$–92) were found, depending on the number of atoms in the cluster, to be either superparamagnetic or with locked-moment component even at room temperature.[8,9] A puzzling increase of the magnetic moment with temperature was also reported. Electronic structure calculations for Gd_{13} clusters predicted[10] canted spin configuration. Recently, it was reported[11] that Dy_N ($N=20$–60) clusters exhibit a nearly antiferromagnetic spin order at about 10 K, although the bulk Dy is ferromagnetic (at this temperatures) with complicated size dependence of magnetic moment.

As mentioned above, due to difficulties in preparation, the studies on RE nanoparticles are limited.[12–18]

The aim of the present work is to produce RE nanoparticles and study their microstructure and magnetic properties. The main issue of the study is to answer the fundamental question whether the observed dramatic modification of the magnetic properties originates from a true size effect or is a manifestation of superparamagnetic behavior, which has been controversially answered in the literature.[14–19]

II. EXPERIMENTAL

Two modifications of the sputtering technique were used, aimed to produce nanoparticles. In the first one, ''multilayer'' precursors of RE (Tb or Gd) and matrix material (Cr or W, for which no alloying with RE is expected according to the bulk phase diagrams) were obtained on a water cooled (100) Si substrate by magnetron sputtering of the corresponding targets. The base pressure of the chamber was 10^{-8} Torr and a high-purity argon gas flow with a pressure of 5 mTorr was used during sputtering. The deposition rate from the RE target was between 1 and 3 Å/s. Two sets of samples were made, in which the thickness of the RE layer was 10 Å and 20 Å, respectively, while the matrix thickness was kept at 10 Å (10/10 and 20/10). The RE nanoparticles were formed by subsequent annealing of the precursors at 600°C. The particle size was controlled by varying the annealing time. In the second modification, the so-called ''continuous mode,'' the atoms were deposited on a substrate continuously rotated above the two targets (RE and matrix material) or by co-evaporation of the RE and matrix material. The speed of the substrate rotation during sputtering was adjusted to ensure RE ''layer'' thickness of less than a few angstroms. This speed was estimated via extrapolating the experimentally found dependence between deposition time and layer thickness. The ratio between the deposited RE and matrix material was estimated to be 20 to 80 at%. In both modifications cover and buffer layers of 200 Å matrix material were used to protect the particles and avoid any effect from the substrate.

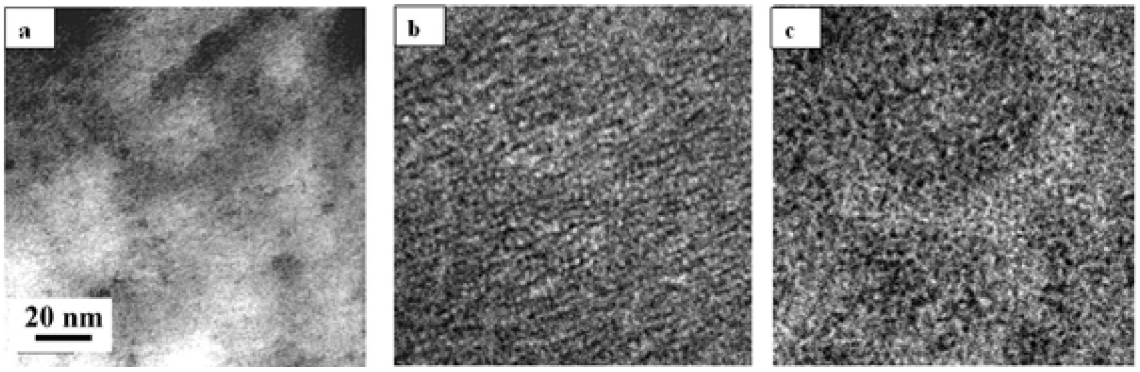

FIG. 1. Energy-filtered images of Tb/Cr (10/10) Å×60 repetitions precursor sample fabricated by the ''multilayer'' mode: (a) Zero-loss image; (b) Cr jump-ratio image; (c) Tb jump-ratio image.

Magnetic properties were measured using both, Superconducting quantum interference device and vibrating-sample magnetometers. The microstructure was examined by conventional TEM (transmission electron microscopy) and SEM (scanning electron microscopy) techniques. To reveal the microscopic features and elemental distribution at the nanometer scale both, energy-filtered imaging and high-resolution-electron microscopy (HREM) were carried out on a Philips CM20 TEM at 200 kV equipped with a Gatan imaging filter.

III. RESULTS AND DISCUSSIONS

A. Structural characterization

The high-resolution electron microscopy and the cross-sectional studies in as-sputtered multilayers reveal an island structure in the layer. The zero-loss image, Cr and Tb jump-ratio images are shown on Fig. 1. The HREM confirmed that the RE islands are isolated (Fig. 2). Subsequent annealing at 600 °C for 20 min results in 3D growth of the islands and to the breaking of the multilayer structure, which is consistent with the results reported by Baberschke.[7] In this way, RE nanoparticles with irregular shape and mean size of about 8 nm are formed. It was found that further increase of the annealing time causes some degradation of the material, due to some oxidation of both the RE and the matrix and, thus, to an effective shrinking of the particles, as found for RE/Cr samples annealed for longer than 40 min. The long annealing time also leads to some alloying between the Si substrate and the buffer layer, as indicated by the microbeam electron diffraction, but no trace of alloying between RE and matrix materials was found. It is worth noting that the RE particle growth is more difficult in W than in Cr matrix, requiring longer time; however, the thermal stability of the former samples is better than the latter. No formation of RE particles was observed in the samples obtained by continuous mode deposition. Composition maps [Figs. 3(a) and 3(c)] show large Cr particles (10–15 nm) coexisting with Tb clusters, which are distributed in the form of networks [Fig. 3(c)]. Electron-diffraction patterns of the continuous mode samples confirm the presence of bcc Cr crystalline phase and an amorphous structure, possibly related to the Tb network clusters. No Tb particles are formed even after annealing at 600 °C for 20 min, implying that for the concentration under study and at the condition used, the mobility of the RE atoms is not sufficient to form particles.

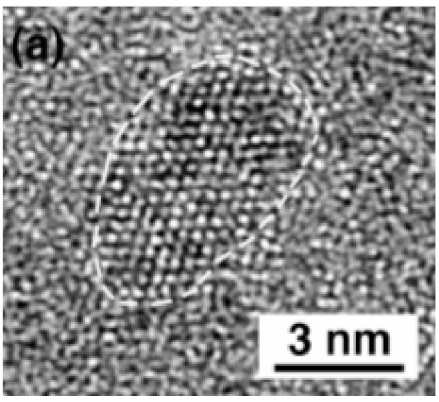

FIG. 2. The HREM image showing a Tb nanoparticle in the Tb/Cr (10/10) Å×60 repetitions precursor sample fabricated by the ''multilayer'' mode.

B. Magnetic properties

In the following, we will discuss mostly the RE/Cr (10/10) Å×60 repetitions based samples (RE=Tb, Gd), while the properties of analogous sample with W as well as samples with 20/10 ratio between RE and matrix material will be given for a comparison. Typical zero-field cooled (ZFC) and field cooled (FC) thermomagnetic curves for particles with mean size of about 8 nm, produced by annealing of multilayer precursors at 600 °C for 20 min, are given on Figs. 4(a) and 4(b) for Tb and Gd, respectively. The M (T) curves show similar features—a magnetization maximum on the ZFC curves, below which a departure between the FC and ZFC magnetization is observed. The temperature of this maximum T_m decreases with increasing the applied field. For Gd an applied field of about 0.2 T is sufficient to suppress the difference between FC and ZFC data, while for Tb this difference persists even in fields as high as 5 T. No peculiarity indicative of a magnetic phase transition has been observed at the characteristic temperatures for bulk Tb (T_N=230 K, T_C=219 K) and Gd (T_C=293 K, T_{sr}=230 K), implying a dramatic decrease of magnetic ordering temperatures

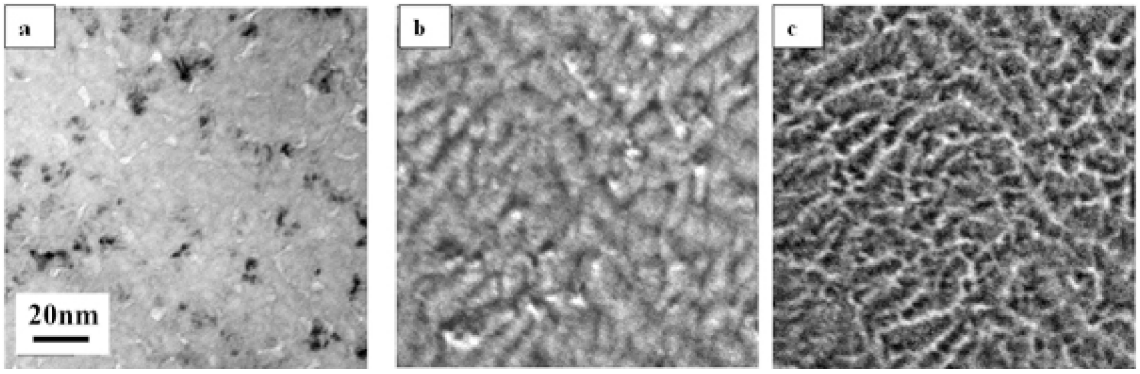

FIG. 3. Energy-filtered of Tb/Cr (10/10) Å×60 repetitions sample fabricated by the ''continuous'' mode: (a) Zero-loss image; (b) Cr jump-ratio image; (c) Tb jump-ratio image.

in the nanosize Tb and Gd particles. This observation is consistent with the results reported by O'Shea[14,15] and Hadjipanayis.[16,17] It is worth noting that nanocrystaline Tb directly passes into a ferromagnetic state contrary to bulk Tb, which orders antiferromagneticaly first with decreasing temperature.

In addition to the type of the magnetic order at low temperatures, a fundamental question arises: whether a true paramagnetic state or a superparamagnetic one is evident at temperatures between T_m and the bulk ordering temperature, i.e., *whether a true size effect takes place*, causing the observed dramatic decrease in the ordering temperature. We believe, that the temperature of magnetization maximum on the zero-field cooled data, T_m, below which the curve departs from the field cooled curve, is attributed to the temperature at which the coercive field is comparable to the applied field rather than to a blocking temperature of superparamagnetic clusters. Below, we will discuss the experiments we have performed and the arguments supporting our statement. We wish to mention that, because of uncertainties in determining the actual mass of the RE in the samples, the attempts to determine the magnetic moments from the susceptibility versus temperature measurements above T_m would be rather speculative and this is the reason why we focus our attention on the low temperature data. As seen from Fig. 5 both, the temperature dependence of coercivity H_c and the field dependence of T_m vary in a similar way. The lower H_c values, compared with the corresponding fields at which the magnetization shows a maximum at certain T_m, can be related to the fact that no saturation is achieved in the range of fields used, as implied from the significant slope of the magnetization curves even at the highest fields used (Fig. 6).

Another support for the relationship between H_c and T_m comes from the fact that for low anisotropy *S*-state Gd the field required to shift T_m below 3 K is about 0.15 *T*, while for the strongly anisotropic Tb, fields as high as 5.5 *T* are not

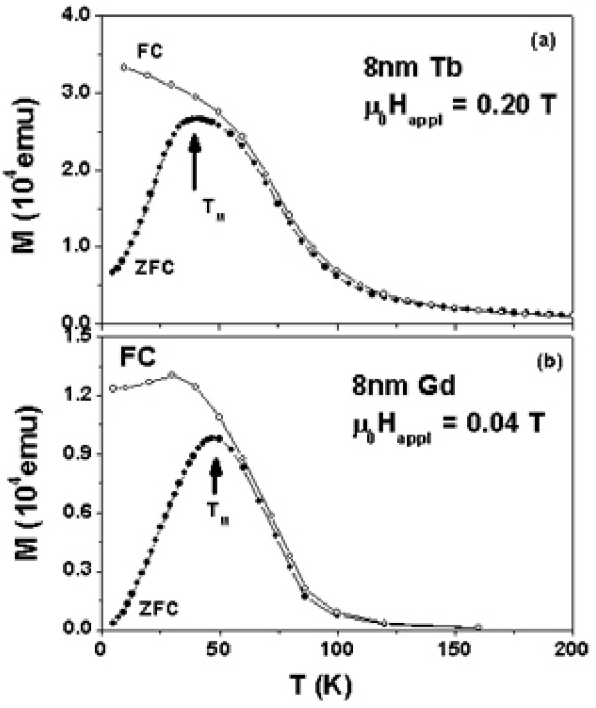

FIG. 4. Field cooled (FC) and zero-field cooled (ZFC) thermomagnetic curves for 8 nm (a) Tb and (b) Gd nanoparticles produced by annealing of R/Cr ''multilayer'' (10/10) Å×60 repetitions precursors at 600 °C for 20 min. The value of the applied field (equal to the cooling field) is given on the plot.

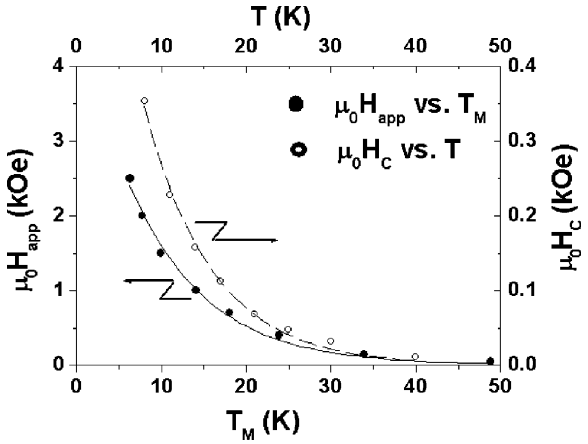

FIG. 5. Temperature dependence of coercivity H_c and field dependence of the temperature of magnetization maximum on the ZFC data, T_m, for 8 nm Tb nanoparticles. The lines are guide for the eye.

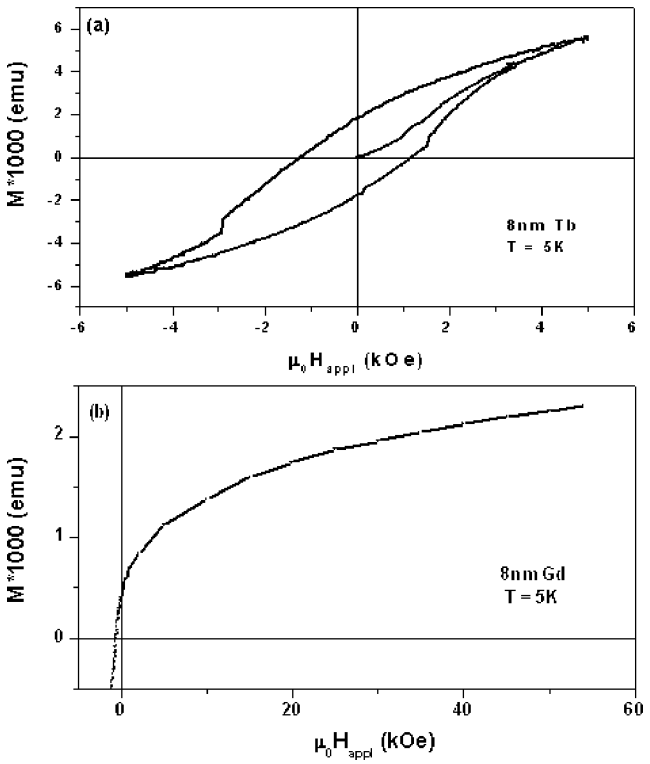

FIG. 6. Hysteresis loops of (a) Tb/Cr (10/10) Å×60 repetitions. (b) Demagnetization curve of Gd/Cr (10/10) Å×60 repetitions multilayer samples, both are annealed at 600 °C for 20 min and nanoparticles of about 8 nm are formed.

sufficient to destroy the maximum at T_m. If alternatively, T_m is manifestation of blocking temperature, for particles with a similar size, one should expect much higher T_m for the non *S*-state Tb (two orders of magnitude higher anisotropy) than for Gd. However, the experimental results for 8 nm mean size Gd and Tb particles show that this is not the case (Fig. 4).

For noninteracting superparamagnetic particles the magnetization curves measured at different temperatures above the blocking temperature are expected to superimpose when plotted against H/T. However, the experimental results do not reveal such behavior regardless whether the matrix material is W or Cr. (Note that in case of Cr the data were corrected for the antiferromagnetic contribution arising from the matrix material by measuring a Cr film with a mass similar to that of the actual sample.)

The size effect hypothesis gains further verification from the relationship between the particle size in the range of 5–20 nm (controlled by the annealing temperature and studied by cross-sectional electron microscopy) and the value of T_m. For short annealing times where no degradation of the samples is observed (below 20 min for Tb/Cr films) the temperature of the ZFC magnetization maximum increases with increasing the annealing time and particles size, respectively, from about 16 K in as-made 1-nm-thick multilayers with island structure to 40 K for particles with size of about 8 nm formed after 20-min annealing. While for the as-made material an increase in T_m is observed when measured in applied field perpendicular to the film plane, no significant difference in the direction of the applied field was observed for the 20-min annealed sample (data not shown). It is natural to attribute this observation to a demagnetizing-field effect, which is strong in the case of elongated and occasionally connected islands in the as-made films and negligible in the case of well separated and more spherically shaped nanoparticles in the annealed samples. This demagnetization field effectively reduces the internal magnetic field and increases T_m in the former material.

It was also found that, in accordance with the discussed relationship between T_m and particle size, an increase of the RE concentration leads to some 50% increase in T_m as observed in the 20:10 RE/Cr samples, both the as made and the annealed samples under the same conditions as the 10:10 samples.

Another demonstration of the size effect is the observed enhancement of coercivity and the slope of magnetization curves reflecting the noncollinear spin structure at the nanoparticles surface. It is worth noting that bulk single crystals of Gd have extremely small coercivity,[20] suggesting the important role of the surface atoms in determining the magnetic properties of RE nanoparticles. We suggest that the coercivity enhancement in the nanoparticles under study is what prevents them from being superparamagnetic, especially in the case of Gd, for which a superparamagnetic behavior is expected above liquid-helium temperatures if the anisotropy is not much different from the bulk anisotropy.

All the samples produced in the continuous mode exhibit paramagnetic behavior in agreement with high-resolution microscopy studies showing that no RE particles are formed but the deposited atoms staying in clusters isolated from each other in the nonmagnetic matrix even after annealing. This result calls for further studies of the percolation limit at which formation of RE nanoparticles and magnetic order can be achieved.

IV. CONCLUSIONS

Isolated Gd and Tb nanoparticles can be obtained via annealing of sputtered multilayer precursors, which themselves are composed of RE islands when produced under the conditions described in this work. A dramatic change in the magnetic characteristics of the nanoparticles is observed when compared to the bulk. The obtained magnetic data gives a credit to the true size effect scenario but not to the superparamagnetic one.

ACKNOWLEDGMENT

This work was supported by the National Science Foundation under Grant No. 9972035.

[1] J.J. Rhyne, in *Science and Technology of Nanostructured Magnetic Materials*, Vol. 259 of *NATO Advanced Studies Institute*, Series B: Physics, edited by G.C. Hadjipanayis and Gary Printz (Plenum, New York, 1991), p. 117.
[2] R.W. Erwin, J.J. Rhyne, M.B. Salamon, J. Borchers, S. Sinha, R. Du, J.E. Cunningham, and C.P. Flynn, Phys. Rev. B **35**, 6808 (1987).
[3] D. Gibbs, P. Boni, A.I. Goldman, J. Kwo M-Hong, T.C. Hsieh, R.M. Fleming, D.B. McWhaan, J.W. Cable, J. Bohr, H. Grimm, and C.L. Cjien, J. Appl. Phys. **63**, 3447 (1988).
[4] H. Li, D. Tian, J. Quinn, Y.S. Li, S.C. Wu, and F. Jona, Phys. Rev. B **45**, 3853 (1992).
[5] D. Weller, S.F. Alvarado, W. Gudat, K. Schrőder, and M. Campagna, Phys. Rev. Lett. **54**, 1 555 (1985).
[6] G. Mulhollan, K. Garrison, and J.L. Erskine, Phys. Rev. Lett. **69**, 3240 (1992).
[7] M. Farle, K. Baberschke, U. Stetter, A. Aspelmeier, and F. Gerhardter, Phys. Rev. B **47**, 11 571 (1993).
[8] D.C. Douglass, J.P. Bucher, and L.A. Bloomfield, Phys. Rev. Lett. **68**, 1774 (1992).
[9] D.C. Douglass, A.J. Cox, J.P. Bucher, and L.A. Bloomfield, Phys. Rev. B **47**, 12 874 (1993).
[10] D.P. Pappas, A.P. Popov, A.N. Anisimov, B.V. Reddy, and S.N. Khanna, Phys. Rev. Lett. **76**, 4332 (1996).
[11] S. Pokrant, Phys. Rev. A **62**, 051201 (2000).
[12] C.E. Krill, F. Merzoung, W. Krauss, and R. Birringer, Nanostruct. Mater. **9**, 455 (1997).
[13] J.A. Cowen, B. Stolzman, R.S. Averback, and H. Hahn, J. Appl. Phys. **61**, 3317 (1987).
[14] D. Johnson, R. Perera, and M.J. O'Shea, J. Appl. Phys. **79**, 5299 (1996).
[15] M.J. O'Shea and P. Perera, J. Appl. Phys. **85**, 4322 (1999).
[16] N.B. Shevchenko, J.A. Christodoulides, and G.C. Hadjipanayis, Appl. Phys. Lett. **74**, 1478 (1999).
[17] J.A. Christodoulides, N.B. Shevchenko, and G.C. Hadjipanayis, Nanostruct. Mater. **12**, 539 (1999).
[18] X.X. Zhang, J. Tejada, J.M. Hernandez, and R.F. Ziolo, Nanostruct. Mater. **9**, 301 (1997).
[19] S.H. Aly, J. Magn. Magn. Mater. **223**, 368 (2000).
[20] S.Yu. Dan'kov, A.M. Tishin, V.K. Pecharsky, and K.A. Gschneidner, Jr., Phys. Rev. B **57**, 3478 (1998).